Cyclic Deformation Response of Ultra-fine Grained Titanium at Elevated Temperatures

S.V. Sajadifar, G.G. Yapici, E. Demler, P. Krooß, T. Wegener, H.J. Maier, T. Niendorf

PII: S0142-1123(18)30508-5
DOI: https://doi.org/10.1016/j.ijfatigue.2019.01.021
Reference: JIJF 4964

To appear in: *International Journal of Fatigue*

Received Date: 7 September 2018
Revised Date: 27 January 2019
Accepted Date: 29 January 2019

Please cite this article as: Sajadifar, S.V., Yapici, G.G., Demler, E., Krooß, P., Wegener, T., Maier, H.J., Niendorf, T., Cyclic Deformation Response of Ultra-fine Grained Titanium at Elevated Temperatures, *International Journal of Fatigue* (2019), doi: https://doi.org/10.1016/j.ijfatigue.2019.01.021

Cyclic Deformation Response of Ultra-fine Grained Titanium at Elevated Temperatures

S.V. Sajadifar[a,c], G.G. Yapici [a,]*, E. Demler[b], P. Krooß[c], T. Wegener[c], H.J. Maier[b], T. Niendorf[c]

[a] Mechanical Engineering Department, Ozyegin University, 34794 Istanbul, Turkey

[b] Institut für Werkstoffkunde (Materials Science), Leibniz Universität Hannover, 30823 Garbsen, Germany

[c] Universität Kassel, Institut für Werkstofftechnik (Materials Engineering), 34125 Kassel, Germany

*Corresponding Author Tel.: +90 216 564 9115; Fax: +90 216 564 9057

E-mail address: guven.yapici@ozyegin.edu.tr

Abstract

This study focuses on the high-temperature cyclic deformation response (CDR) of ultra-fine grained (UFG) Ti of commercial purity (grade 4) processed via equal channel angular extrusion as a severe plastic deformation method. Low-cycle fatigue experiments were conducted at elevated temperatures up to 600 ^{o}C and at strain amplitudes ranging from 0.2% to 0.6%. Besides temperature and strain amplitude, the influence of two processing routes ($8B_C$ and 8E) on the fatigue characteristics of UFG Ti was examined. It is clearly revealed that the CDR of UFG Ti is not strongly affected by the alteration of strain path during ECAE processing, as long as highly efficient routes are employed. Both routes lead to high volume fraction of high angle grain boundaries and improved fatigue performance up to 400 ^{o}C is demonstrated. Electron backscatter diffraction assisted microstructural characterization was used to analyze elementary degradation mechanisms affecting cyclic mechanical behavior. Micrographs reveal the occurrence of severe recrystallization and grain growth only at temperatures above 400 ^{o}C and,

thus, grade 4 UFG Ti is characterized by unprecedented cyclic stability in comparison to other UFG alloys.

Keywords: Titanium; Ultra-fine Grained; Severe Plastic Deformation; Fatigue; Cyclic Stability; Elevated Temperature

1. Introduction

Commercial purity titanium (Ti) attracted great interest within recent decades [1–8]. Specifically, ultra-fine grained (UFG) Ti has shown an outstanding biocompatibility along with a high strength to density ratio [1]. Titanium is one of the few metals meeting the requirements for implantation in the human body, however, a relatively low strength of this material limited its applicability in this particular field as well as other engineering applications demanding superior corrosion performance. Hence, UFG Ti due to its high strength shows an excellent potential for application not only in the biomedical sector but also in e.g. the mobility sector and chemical industry. From numerous studies in the field of UFG alloys it is well known that microstructural stability of UFG materials under thermal and/or cyclic plastic loadings, i.e. in the LCF regime, can be strongly deteriorated [9–14] eventually leading to inferior properties as compared to coarse grained counterparts. In order to qualify the grade 4 UFG Ti alloy for any kind of demanding application in such fields, the worst case scenario, i.e. LCF loading at elevated temperature, has been considered in the present study. By this, outermost limits of microstructural stability are deduced. Various techniques such as rapid solidification, mechanical alloying and severe plastic deformation (SPD) have been introduced in order to manufacture UFG Ti [15]. Among these approaches, SPD was identified to be the most

promising for obtaining UFG microstructure and eventually strength improvement [5,6]. The most commonly utilized SPD methods are equal channel angular extrusion/pressing (ECAE/P), high pressure torsion (HPT) and accumulative roll bonding (ARB) [2–4]. As the most notable SPD method for obtaining fairly large samples, several studies have focused on effects of ECAE processing routes on the microstructure and mechanical properties of commercial purity Ti [4]. Accordingly, route E and B_c were reported to be favorable for processing hcp Ti as these routes resulted in the largest fully worked region with high volume fraction of high-angle grain boundaries (HAGB).

High-temperature deformation of UFG Ti has only recently become the subject of research [16–20]. Specifically, tensile strength and microstructure evolution of grade 2 titanium processed by ECAE and followed by rolling have been studied in the temperature range of 300 °C to 500 ^{o}C [16]. Up to 500 ^{o}C, strength upon SPD remained higher in comparison to non-processed, coarse-grained reference material, although UFG materials are prone to thermally driven coarsening. Furthermore, the monotonic response of this material was examined up to 650 ^{o}C [17]. At deformation temperatures above 500 ^{o}C, the strength of UFG Ti decreased to the level of coarse-grained (CG) Ti due to recrystallization and/or thermally-induced grain growth. Workability and hot deformation characteristics of severely deformed Ti were also investigated at temperatures ranging from 600 ^{o}C to 900 ^{o}C employing various strain rates [17,19]. High temperature workability was analyzed based on the flow localization parameter and deformation at and below 700 ^{o}C was found to be prone to localization. At deformation temperature of 500 ^{o}C, UFG Ti exhibited superplastic behavior [20]. This superplastic behavior

stemmed from the grain boundary sliding by the improvement in the strain rate sensitivity of the flow stress.

The necessity of evaluating the fatigue properties for envisaged applications has shaped interest towards characterization of the cyclic deformation response. Therefore, some attempts to analyze the fatigue response of UFG Ti at ambient temperature were carried out [21–24]. A considerable increase in fatigue life and fatigue limit under constant load in UFG Ti was reported [21]. Cyclic response of severely deformed materials was rationalized by Hall-Petch grain boundary hardening and dislocation hardening. High-cycle fatigue behavior of this material has also been studied [22]. ECAE processing caused an increase in the fatigue endurance limit of titanium, while SPD worsened notch sensitivity of this material due to a pronounced decrease in the characteristic microstructural length that governs crack growth. Meanwhile, thermo-mechanical treatment was conducted on UFG Ti to improve its ductility and notch sensitivity [23]. Investigation of the low-cycle fatigue (LCF) characteristics of UFG Ti at room temperature provided key insight in the impacts of grain refinement on the cyclic response and cyclic stability [24,25]. The LCF life of UFG Ti was found to be longer than that of CG Ti in both studies. However, UFG samples of different orientations demonstrated varying fatigue lives and stress ranges due to both texture and oriented sub-grain boundaries [25].

LCF behavior at elevated temperatures has not been comprehensively examined for severely deformed titanium, yet. The investigation of fatigue behavior and thermal stability of UFG Ti is crucial to provide guidelines and stability limits for engineering and medical applications. Various mechanisms e.g. deformation-induced, thermal-induced and deformation-induced thermally activated grain growth might be responsible for changes in fatigue

performance of UFG materials during cyclic deformation at elevated temperature [26,27]. In order to close this gap, this paper investigates the cyclic stability of ECAE processed commercial purity titanium processed by two different ECAE routes and reveals elementary microstructural degradation mechanisms. For this purpose, the CDR and microstructural evolution of severely deformed grade 4 titanium at different temperatures (up to 600 ^{o}C) and various strain amplitudes are presented. It is revealed that the microstructural conditions tested are characterized by unprecedented stability under the given loading conditions. The results obtained open up new pathways for the development of superior UFG materials.

2. Experimental Procedure

The commercial purity grade 4 Ti was received in form of bars with lengths of 100 mm and cross sections of 25.4 mm × 25.4 mm and with the chemical composition listed in Table 1. Before extrusion, the bars were coated with a graphite base lubricant and subsequently heated in a furnace to the deformation temperature where they were held for 1 h. The minimum deformation temperature that allowed for processing without shear localization and macroscopic cracking for a 90^{o} ECAE die was determined to be 450 ^{o}C. Minimization of processing temperatures was crucial in order to prevent potential recrystallization and partly achieved using the sliding walls concept [28]. Extrusion took place at a rate of 1.27 mm/s. Eight ECAE passes were performed following routes E and B_C, respectively, accumulating a total strain of 9.24 in the as-processed material. Route E, a so called hybrid route, consists of an alternating rotation of the billet by +180^{o} and +90^{o} around its long axis, while in route B_C the billet was always rotated by +90^{o} around its long axis between each successive pass [19]. Following each

extrusion pass, the billets were water quenched to maintain the microstructure achieved during ECAE.

Table 1. Chemical composition of the grade 4 titanium used in this study

Element	C	Fe	H	N	O	Ti
weight percent (%)	0.012	0.206	0.0028	0.009	0.30	Balance

LCF experiments were conducted using flat dog-bone shaped samples with gage sections of 20 mm × 5 mm × 1.5 mm and 8 mm x 3 mm x 1.5 mm for the elevated and room temperature tests, respectively. All samples were electro-discharge machined (EDM) with their axis parallel to the extrusion direction. All samples were ground and polished to remove major scratches and eliminate the influence of the residual layer from EDM. Cyclic tests were carried out under isothermal conditions at three different strain amplitudes of 0.2%, 0.4% and 0.6% and at temperatures of 25 ^{o}C, 400 ^{o}C and 600 ^{o}C. An MTS 793 servo-hydraulic test frame was used to perform the fatigue experiments. All LCF tests were conducted in total strain control under a nominal strain rate of 0.006 s^{-1}, i.e. triangular type loading, resulting in testing frequencies ranging from 0.25 to 0.75 Hz. Fatigue experiments were carried out under fully reversed constant total strain amplitude (R = -1) conditions. A high-temperature extensometer with ceramic rods was used to measure strains during cyclic tests at elevated temperatures. Strain measurement in the RT tests was achieved by using a miniature extensometer with a 3 mm gauge length directly attached to the sample surfaces.

Optical microscopy was used to monitor the changes in the microstructure. The specimens were prepared using standard polishing techniques and then etched with Kroll's reagent.

Scanning electron microscopy (SEM) at a nominal acceleration voltage of 20 kV and electron backscatter diffraction (EBSD) were utilized to study details in microstructure evolution of specimens in different conditions. For EBSD examination, the samples were prepared by 4 hours of vibropolishing in a colloidal silica solution.

3. Results and Discussion

3.1. Cyclic Response of UFG and CG Ti at Room Temperature

Tensile properties of CG and UFG Ti are summarized in Table 2. ECAE processing could remarkably improve the strength levels of Ti without deteriorating ductility. The enhancement of strength can be linked to the grain boundary strengthening.

Table2. Summary of the results of the tensile experiments performed at ambient temperature on UFG and CG Ti

Condition	Yield Strength (MPa)	UTS (MPa)	Fracture Strain (%)
CG Ti	531 ± 6	792 ± 9	25 ± 2
Route-8E UFG Ti	758 ± 8	947 ± 13	25 ± 3
Route-8B$_c$ UFG Ti	812 ± 10	989 ± 15	17 ± 3

Figure 1 shows the evolution of cyclic stress versus the number of cycles at various strain amplitudes (Fig. 1a) and half-life hysteresis loops for CG and route-8E processed UFG Ti at ambient temperature (Fig. 1b). Generally, fatigue life and cyclic stability of both UFG and CG Ti are degraded with the increase of strain amplitude. It is well-known that fatigue crack initiation and propagation are promoted by increased strain amplitude [29]. Similar cyclic deformation

behavior was also reported for the Ti alloy IMI 834 [30]. At the same strain amplitude, UFG Ti shows higher fatigue life and stress range levels than the CG material. Higher stress range for UFG Ti is strongly promoted with increasing strain amplitude, concomitantly the fatigue life is slightly reduced. By considering the half-life hysteresis loops as depicted in Fig. 1b, fatigue behavior can be analyzed in more detail. The area of a hysteresis loop is a measure for energy dissipation per cycle. It is well-known that higher energy dissipation per cycle is linked to more intense dislocation activity, eventually leading to crack nucleation [31].

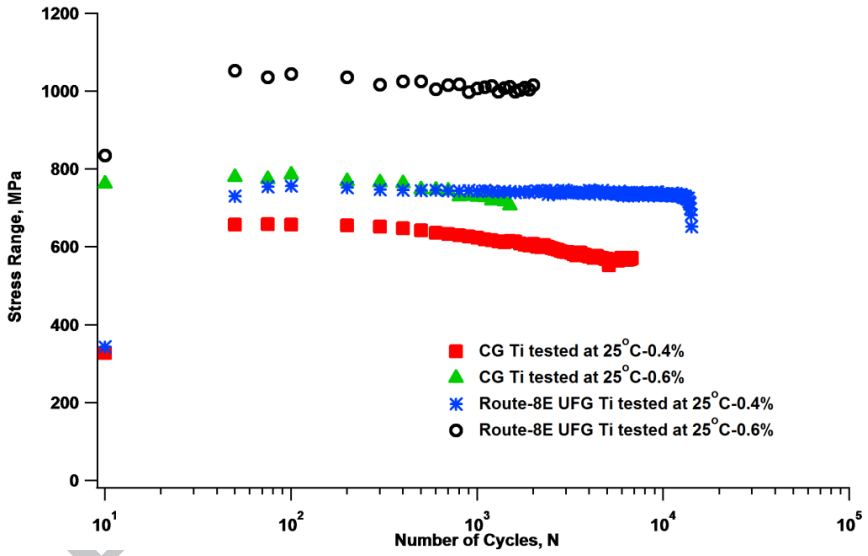

(a)

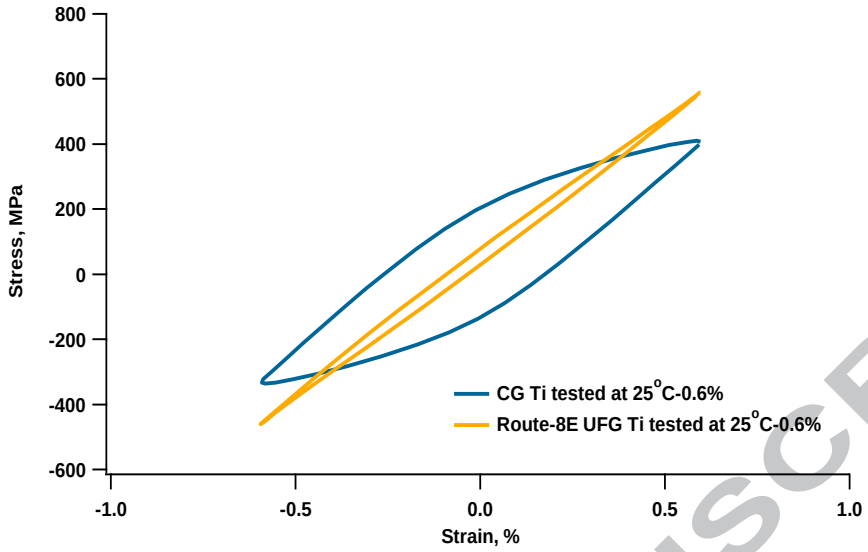

(b)

Figure 1. (a) CDR of CG and UFG Ti at ambient temperature; (b) half-life hysteresis loops of CG and UFG Ti at ambient temperature and a strain amplitude of 0.6%

The large differences in the areas of the hysteresis loops are clear indications of minimized energy dissipation per cycle for the UFG Ti. Reason for this is seen in the superior strength induced by grain refinement in the UFG material (cf. Table 2). From the width of the hysteresis loop the plastic strain range can be deduced. As expected from the increased monotonic strength and as already was shown for grade 2 UFG Ti, plastic strain range in the LCF regime is significantly decreased for the UFG conditions considered here, eventually leading to the superior fatigue response, i.e. highest stress ranges and fatigue lives.

3.2. Cyclic Response of UFG and CG Ti at Elevated Temperature

The stress range-fatigue life curves of both UFG and CG Ti at 400 ^{o}C and 600 ^{o}C are displayed in Fig. 2. It is evident that the cyclic stabilities of both UFG and CG Ti are sensitive to temperature and strain amplitude. Furthermore, it can be seen that for all strain amplitudes employed, UFG Ti exhibits higher stress range levels than the CG Ti at 400 ^{o}C. This is more apparent for the higher strain amplitudes of 0.4% and 0.6%. By contrast, CG Ti surpassed UFG Ti at the higher temperature of 600 ^{o}C (Fig. 2b). Higher stress range levels of UFG materials during LCF can be imputed to their decreased grain size and higher volume fraction of HAGBs, respectively, hindering the movement of dislocations efficiently [25]. However, elevated temperatures facilitate the occurrence of recrystallization and grain growth leading to a decrease of strength [17]. A study on UFG interstitial free (IF) steel showed that its UFG structure remains thermally stable up to 500 ^{o}C under pure thermal loading. However, stress range levels and fatigue lives considerably decreased at high temperatures, whereby significant reduction of fatigue life was already seen at a temperature of 300 °C [9]. Similarly, fatigue lives of both UFG and CG Ti drop with the rise of homologous temperature (T_h), however, up to 400 °C stability of CDR is hardly affected. It is well-documented that cyclic stability of UFG materials is negatively influenced by exposure to temperatures above a critical T_h value [32-35]. This value was reported as 0.20, 0.26, 0.32 and 0.40 for UFG copper, UFG IF steel, UFG NbZr and UFG AlMg alloy, respectively. As mentioned before, UFG Ti remains stable up to 400 ^{o}C, whereas, thermal instability with low stress range levels was observed only at 600 ^{o}C. The temperature of 400 °C corresponds to a homologous temperature of 0.35.

To study the impact of strain amplitude on the CDR, three amplitudes of 0.2%, 0.4% and 0.6% were selected. The results demonstrate that both stress range and fatigue life show a

strong dependence on strain amplitude (Fig. 2). Accordingly, UFG and CG Ti could tolerate higher cycle numbers at lower strain amplitudes. This was previously rationalized in terms of impurity assisted grain boundary stabilization, which was mentioned for UFG Ti and other materials [10,12,25,35]. At 400 ^{o}C and a strain amplitude of 0.2%, fatigue life of UFG Ti was seen to reach over 85,000 cycles, while the CG structure withstood less than 16,000 cycles. Remarkably, LCF experiments on UFG Ti at 400 ^{o}C with strain amplitudes of 0.4% and 0.6% resulted in cyclic hardening followed by subsequent softening and cyclic instability. The latter can be ascribed to the occurrence of various damage mechanisms as elaborated in the next section. The transient behavior in the initial cycles, already seen in UFG IF steel fatigued at elevated temperature [9], is thought to be related to strain path changes and a re-arrangement of the dislocation arrangement. Experimental proof, however, is beyond the scope of the current study.

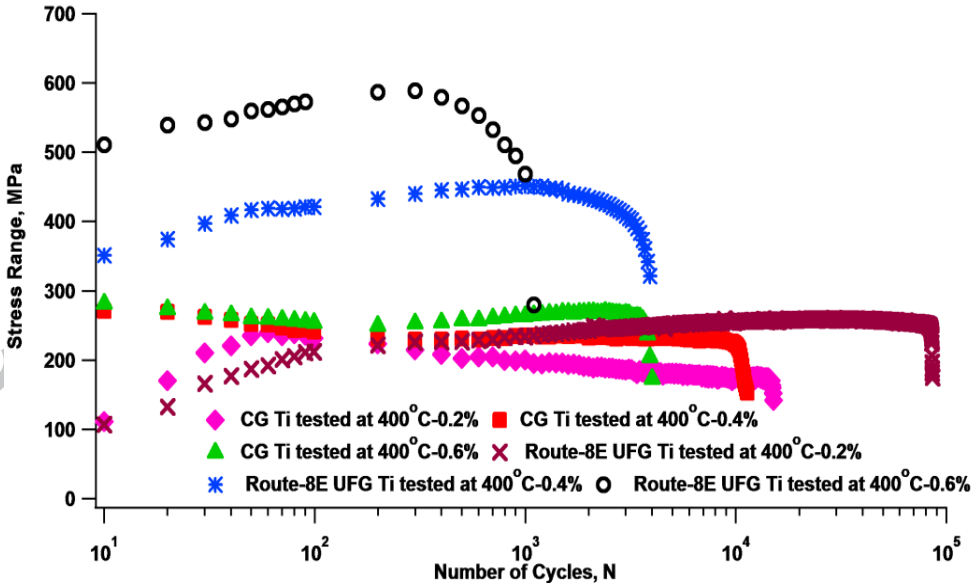

(a)

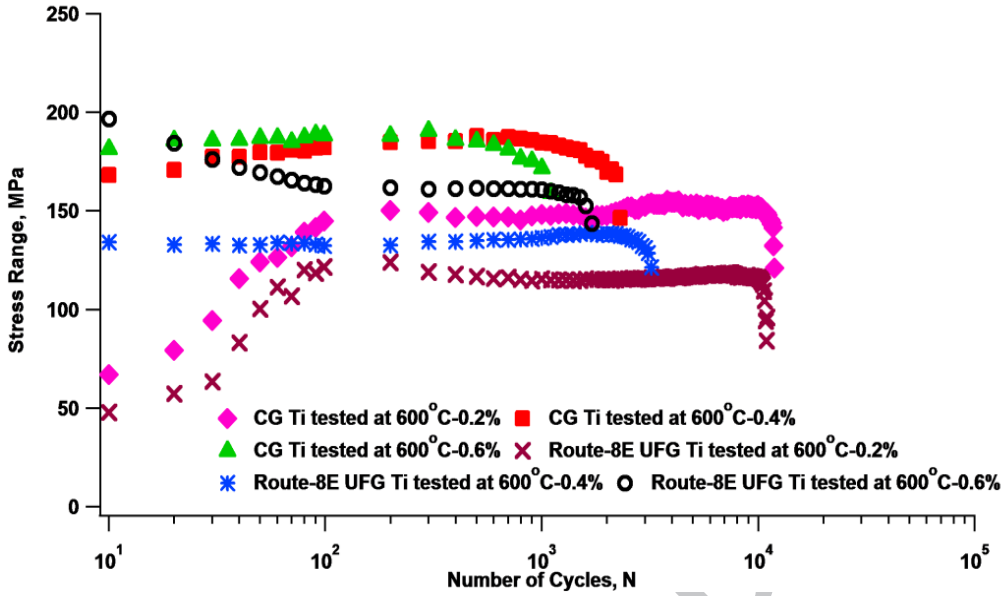

(b)

Figure 2. CDR of CG and UFG Ti at (a) 400 °C and (b) 600 °C

It is also important to elaborate the course of the cyclic transient behavior during cyclic deformation. UFG Ti exhibits a stable CDR especially at relatively low strain amplitudes, while the cyclic softening is evident for the case of CG material. Such cyclic stability was already reported to be linked to the immobilization of grain boundaries via impurities [25]. As a result, grain coarsening can be delayed or hindered during cyclic deformation.

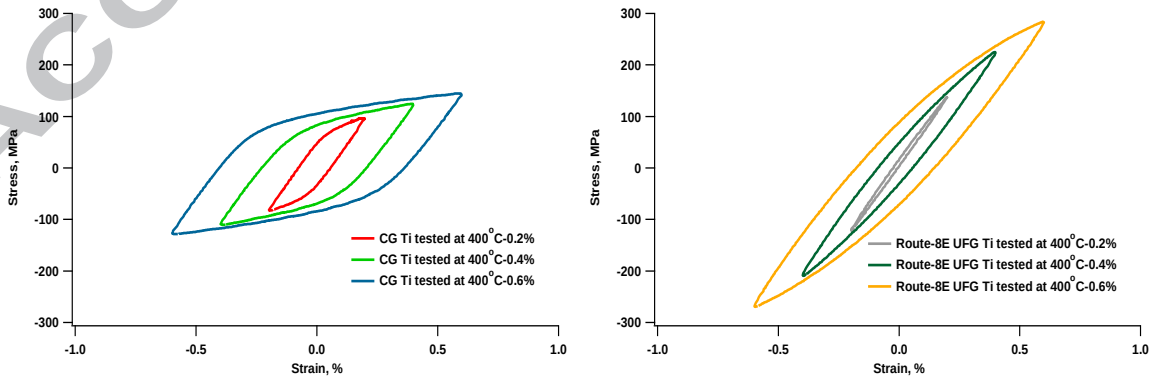

(a) (b)

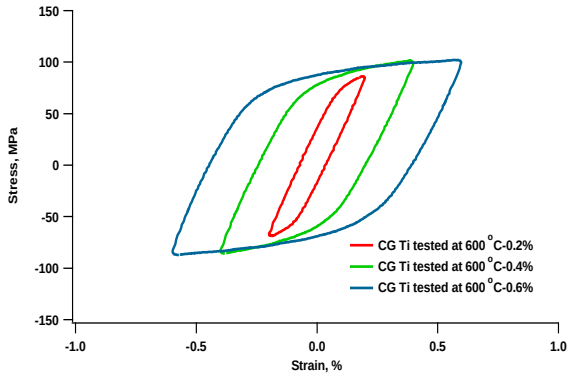

(c)

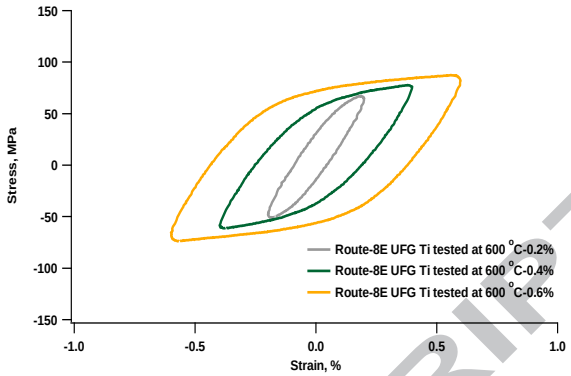

(d)

Figure 3. Half-life hysteresis loops of (a) CG Ti at 400 °C, (b) Route-8E UFG Ti at 400 °C (c) CG Ti at 600 °C and (d) Route-8E UFG Ti at 600 °C

Figure 3. represents the half-life hysteresis loops of CG and UFG Ti at elevated temperatures. It can be seen that the loops of both CG and UFG Ti are symmetrical. Regardless of the grain size, stress range values noticeably increase with the rise of strain amplitude. Similar symmetrical half-life hysteresis loops were also reported for Ti alloys during room temperature fatigue experiments [36,37]. It is also noteworthy that at 400 °C, the area of UFG Ti hysteresis loops is significantly less than that attained for CG Ti samples. On the other hand, at 600 °C UFG Ti demonstrates a similar hysteresis behavior as the CG counterpart. These observations are in accordance with the superior fatigue performance and high stress range levels of UFG Ti up to 400 °C.

3.3. Microstructural Evolution

SEM micrographs utilizing back-scattered electron (BSE) contrast are shown in Fig. 4. These micrographs provide information on the CG and UFG microstructures. Most importantly, 8

passes of ECAE processing was capable of transforming the initial CG structure into UFG material. The average grain sizes of CG and UFG Ti were measured to be 46 μm and 300 nm, respectively. The BSE micrograph of UFG Ti was captured from the longitudinal plane, grain size distributions on other planes were similar (not shown for the sake of brevity).

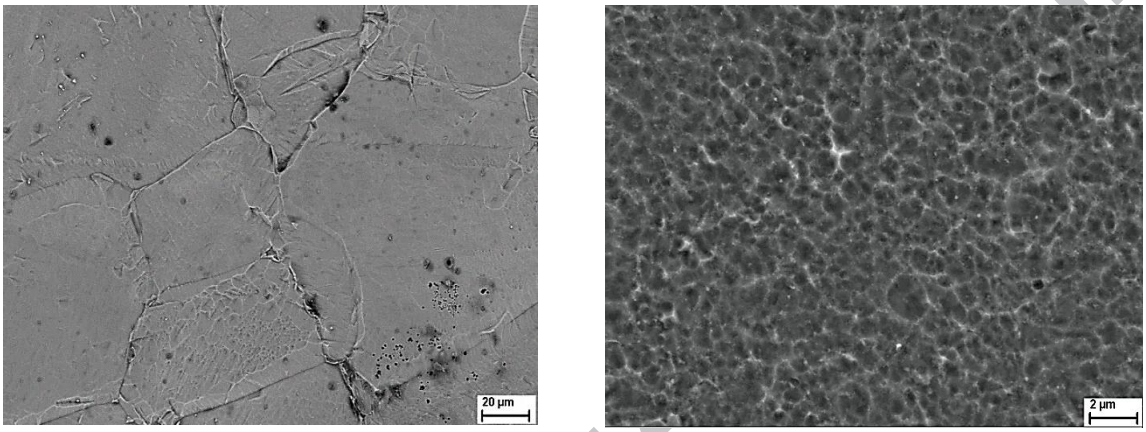

(a) **(b)**

Figure 4. . Micrographs revealing microstructural details using BSE contrast (a) CG Ti, (b) Route-8E UFG Ti

Optical micrographs of UFG Ti subjected to cyclic loading at 400 ^{o}C and 600 ^{o}C with strain amplitudes of 0.2% and 0.4%, respectively, are presented in Fig. 5. The images were captured in the vicinity of fatigue cracks. It is obvious that the microstructure of the UFG Ti sample fatigued at 400 ^{o}C still consists of regions with ultra-fine grains (Fig. 5a). In contrast, as demonstrated in Fig. 5b, recrystallization and grain growth took place in the severely deformed Ti sample under cyclic loading at 600 ^{o}C. It is documented in literature that the movement of grain boundaries, as the main mechanism of grain growth, is facile at such a high homologous temperature [19,38].

In order to study the influence of ECAE processing on the fracture behavior of UFG titanium after cyclic loading, SEM studies were carried out. The fracture surfaces of the severely deformed titanium tested in the LCF experiments at various temperatures are shown in Fig. 5c-f. The micrographs were captured to reveal the fatigue crack propagation zone. Typical fracture surfaces including striations and beach mark patterns are revealed for both deformation temperatures. The striation observed on the fracture surfaces were taken at stable crack growth regions. Generally, the fatigue crack propagation zone is distinguished by the aforementioned striations that are perpendicular to the crack growth direction [39-42]. It can also be noticed that cyclic loading at higher temperatures resulted in coarser fatigue striations. Kitahara *et al*. reported a similar striation pattern for fatigue crack growth experiments of UFG titanium processed via ARB [43]. Higher striation spacing is an indication of higher crack growth attesting better fatigue performance of titanium with ultra-fine grains.

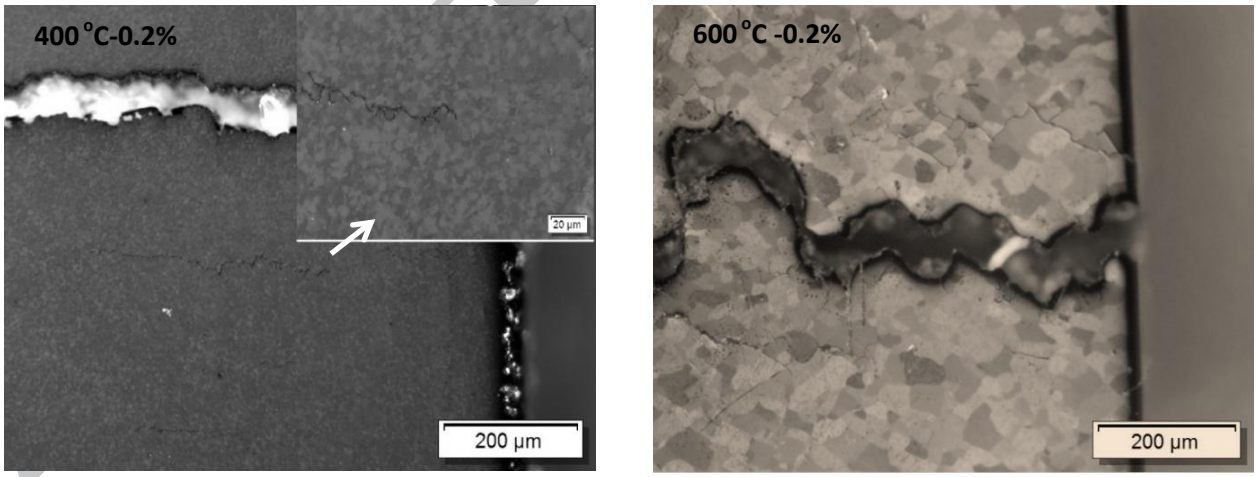

(a) **(b)**

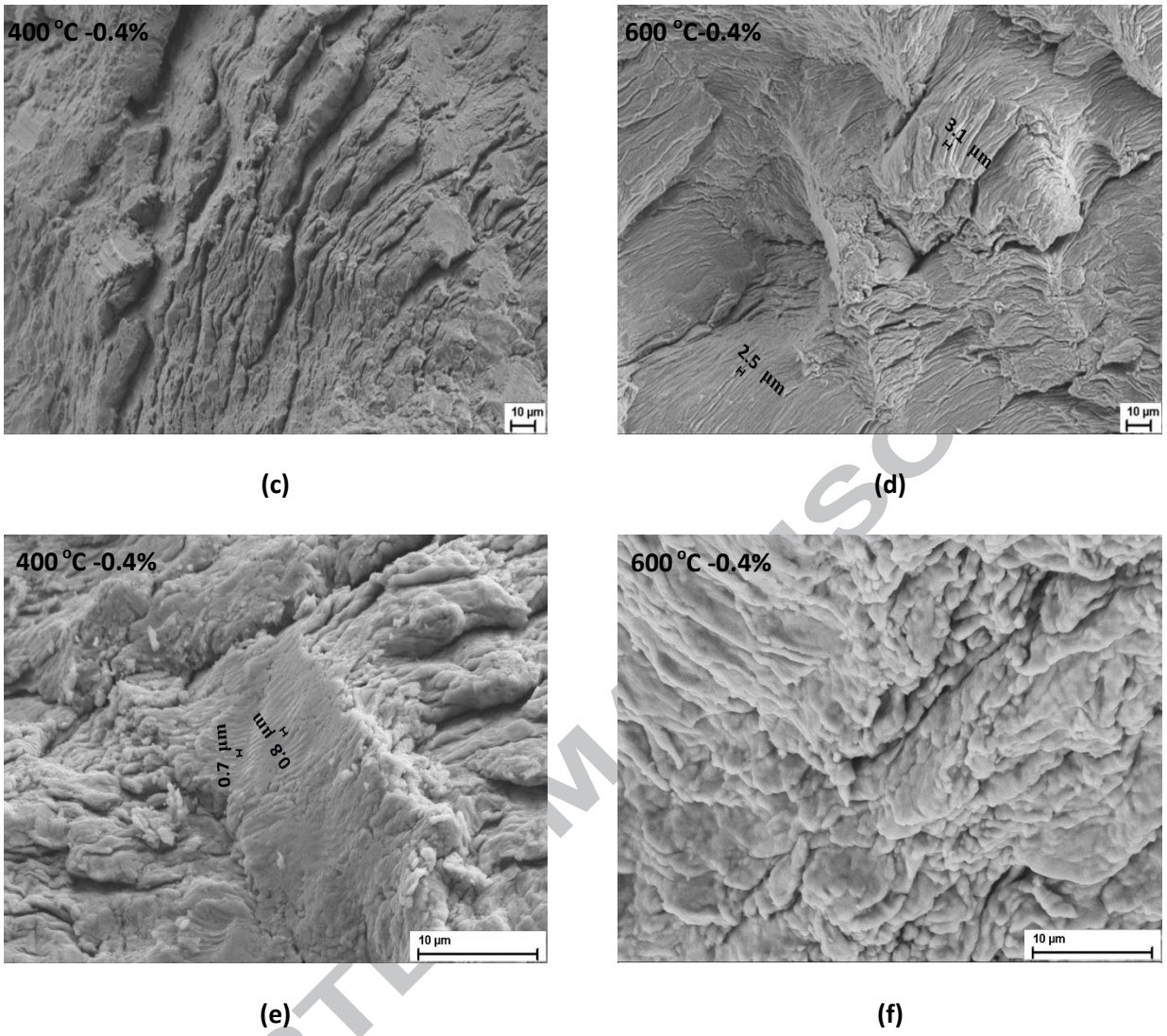

Figure 5. Optical micrographs in the vicinity of fatigue cracks in UFG Ti following cyclic loading (a) at 400 °C at a strain amplitude of 0.2% with high magnification inset, and (b) at 600 °C at a strain amplitude of 0.2%; SEM images of fracture surfaces of samples fatigued (c) and (e) at 400 °C at a strain amplitude of 0.4% (distance from the crack origin is 0.3 mm) and (d) and (f) at 600 °C with strain amplitude of 0.4% (distance from the crack origin is 0.4 mm); (e) and (f) were recorded at high magnification. See text for details

EBSD orientation maps and corresponding misorientation distribution histograms of severely deformed Ti after cyclic tests at elevated temperatures are provided in Fig. 6. From Fig. 5a and 6a it can be followed that the sample cyclically deformed at 400 ^{o}C employing a strain amplitude of 0.2% is still characterized by an ultra-fine grained microstructure. However, the sample subjected to LCF at 600 ^{o}C shows a microstructure with remarkably large grains in comparison with those of the fatigued sample at 400 °C (Figs. 5b, 6b and 6e). Grain growth occurs following common softening mechanisms such as static and dynamic recrystallization (DRX) in order to reduce the internal energy of the structure [44]. EBSD observations align well with the corresponding cyclic response of UFG Ti at different temperatures, i.e. the better cyclic performance of UFG Ti at 400 ^{o}C is imputed to the stability of the microstructure.

The influence of increased strain amplitude was also explored via EBSD. Interestingly, a higher strain amplitude at 400 ^{o}C led to the formation of a bimodal microstructure, i.e. a combination of CG and UFG regions (Fig. 6c). It is well-known that high strain amplitudes and moderate temperatures can result in localized grain growth in UFG microstructures [9]. Basically, different mechanisms e.g. deformation-induced, thermal-induced and deformation-induced thermally activated grain growth are defined to be responsible for coarsening of severely deformed metallic materials [26,27,45,46]. Since 400^{o}C is considerably lower than the temperature to trigger recrystallization and subsequent grain growth for Ti, deformation-induced thermally activated grain growth is thought to be the dominant mechanism for observing such an abnormal coarsening for the sample cyclically deformed at 400 ^{o}C with strain amplitude of 0.6%. Previous studies on nanocrystalline Ni showed that strain/stress-induced abnormal grain growth (AGG) strain-induced AGG could be thermally assisted [47]. In the

current study these large grains are thought to cause localized damage and adversely affect fatigue performance, promoting decreased fatigue lives of UFG Ti at 400 ^{o}C tested with strain amplitudes above 0.2% (Fig. 2a). At 600 ^{o}C and a strain amplitude of 0.6%, grain growth in the whole structure took place. It is assumed that due to the higher amount of strain, dynamically recrystallized grains are relatively finer than those observed for the sample fatigued at 0.2%. This is in line with findings reported in literature, where increasing stress levels indeed lead to a reduction of DRX grain size at high strains [48].

Grain boundary misorientation distribution as deduced from EBSD analysis (not shown) revealed the efficiency of grain refinement by ECAE route 8E. The major fraction of grain boundaries was of the high-angle type. Here, boundaries with misorientation angle less than 15^{o} are considered as low-angle grain boundaries (LAGB). Studies on interstitial free steel demonstrated that a high fraction of HAGBs is crucial to promote cyclic stability of UFG materials [12]. This stability stems from the fact that HAGBs are hardly rearranged via interactions with dislocations under cyclic deformations. Overall, these microstructural findings further rationalize the stable cyclic deformation response of UFG Ti up to the temperature of 400 °C (Fig. 2, 3 and 6).

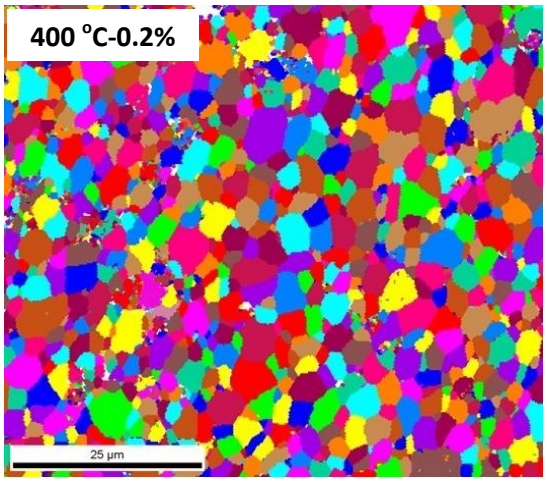
400 °C-0.2%
25 µm

(a)

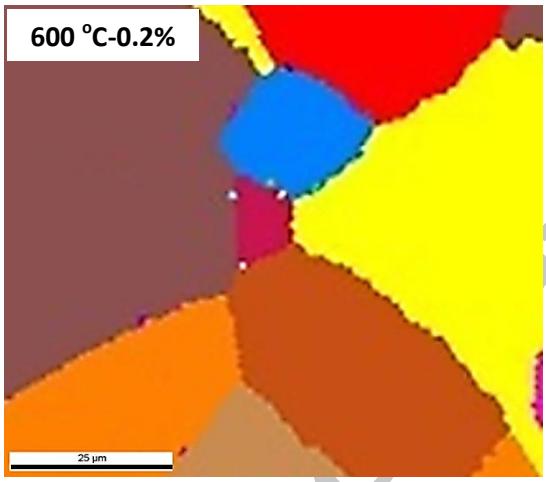
600 °C-0.2%
25 µm

(b)

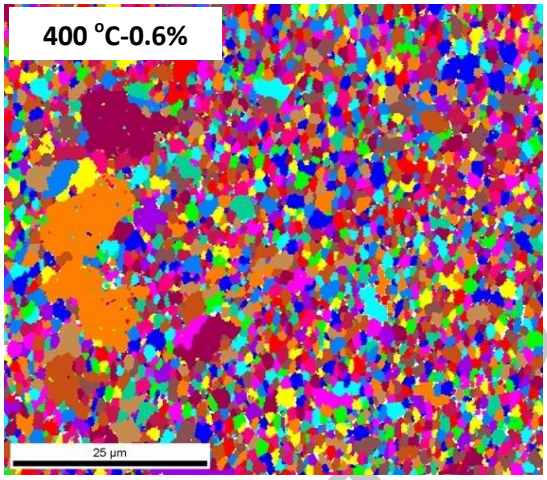
400 °C-0.6%
25 µm

(c)

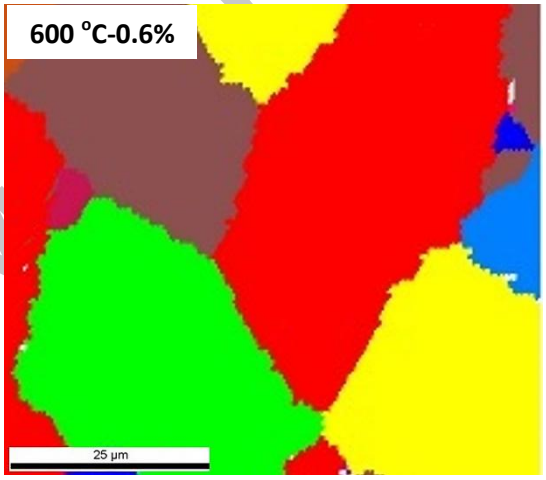
600 °C-0.6%
25 µm

(d)

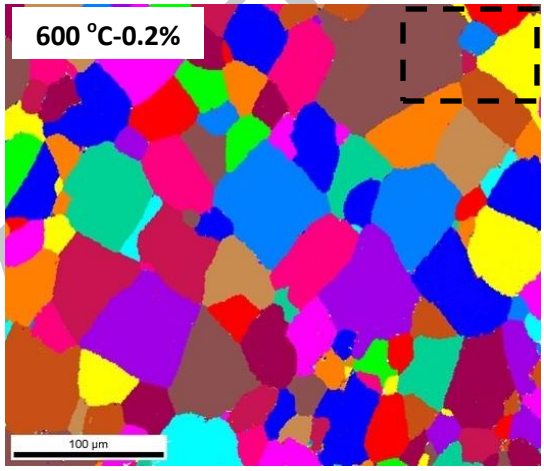
600 °C-0.2%
100 µm

(e)

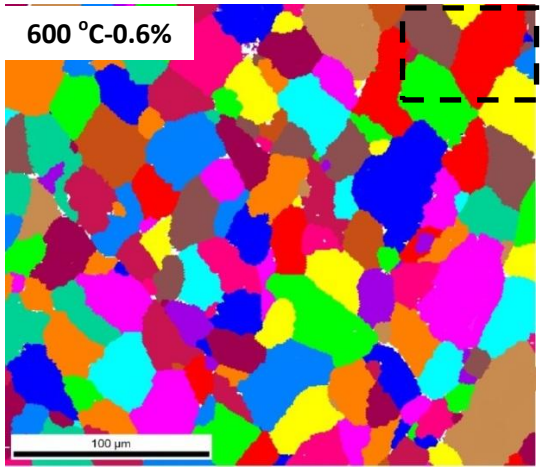
600 °C-0.6%
100 µm

(f)

Figure 6. EBSD images of UFG Ti following cyclic loading at (a) 400 ^{o}C with strain amplitude of 0.2% (b) and (e) 600 ^{o}C with strain amplitude of 0.2% (c) 400 ^{o}C with strain amplitude of 0.6% and (d) and (f) 600 ^{o}C with strain amplitude of 0.6%.

3.4. Effect of ECAE Route on the Cyclic Behavior

This section focuses on the effects of two ECAE processing routes (E and B_c) on the resulting mechanical behavior of grade 4 UFG Ti at elevated temperatures. Prior to loading, thermal stability of 8E, 8B_c and CG Ti was determined by microhardness measurements after 1h annealing at various temperatures (Fig. 7). Hardness values were found to be independent of the ECAE routes employed. A decrease in hardness of UFG Ti is seen at 600 ^{o}C, attesting the occurrence of recovery and recrystallization of the UFG structure at such a high homologous temperature. From Fig. 7, a temperature of 500 ^{o}C can be recognized as a limit for thermal stability of UFG grade 4 Ti under pure thermal loading.

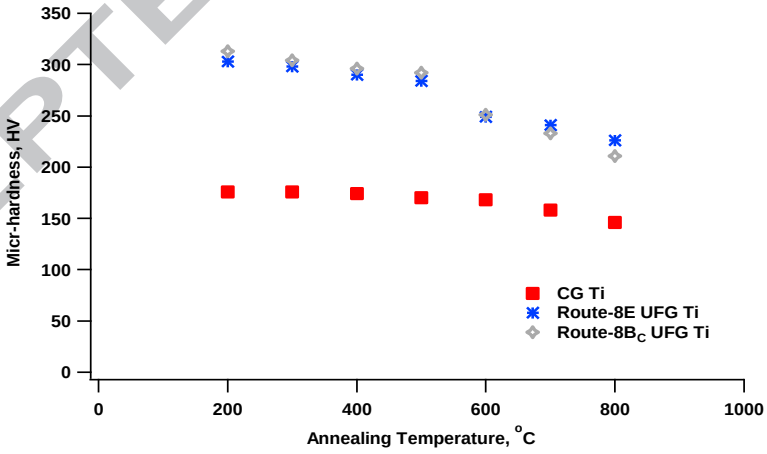

Figure 7. Microhardness evolution as a function of annealing temperature for a dwell time of 1 h

Room temperature CDR of route-8E UFG Ti, route-8B_c UFG Ti and CG Ti are displayed in Fig. 8. As expected, the fatigue performance of UFG Ti processed via route-8E and route-8B_c surpasses that of CG Ti. A slight difference in cyclic stability of route-8E and route-8B_c UFG Ti can also be deduced from Fig. 8. Particularly, route-8B_c shows higher fatigue life and stress range values. This can be ascribed to the formation of a higher fraction of equiaxed fine grains and HAGBs, respectively, in materials processed via route-B_c [4].

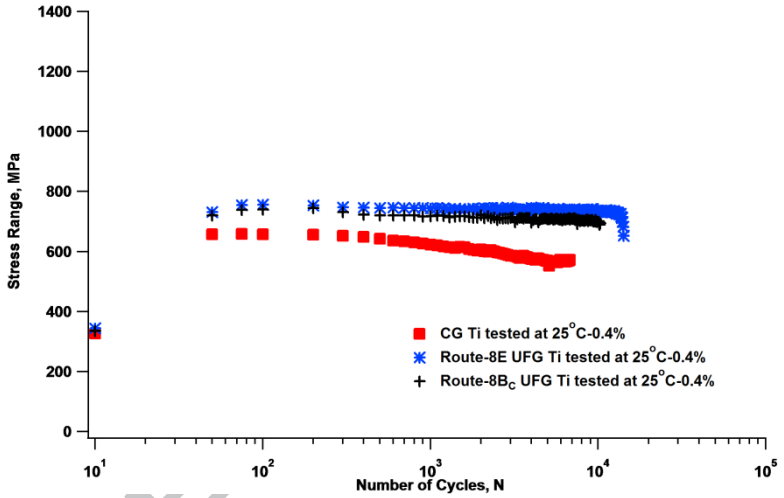

(a)

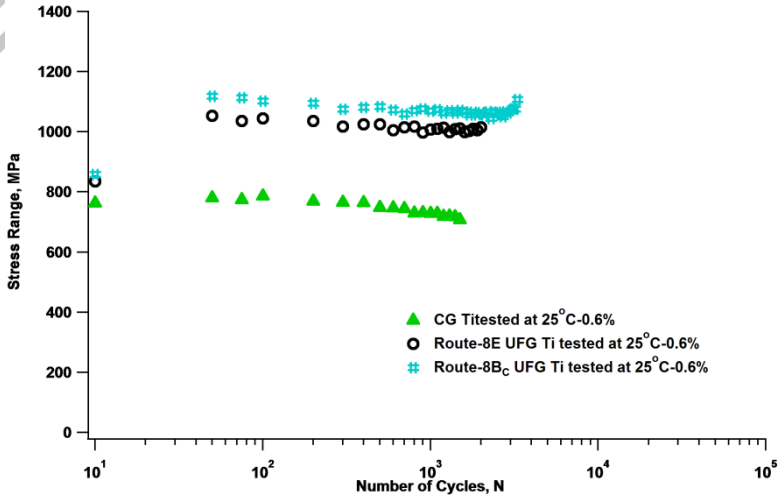

(b)

Figure 8. CDR of CG Ti, route-8E and route-8Bc UFG Ti at room temperature with strain amplitude of (a) 0.4% and (b) 0.6%

Figure 9 depicts the CDR plots of route-8E UFG Ti, route-8B_c UFG Ti and CG Ti samples tested at 400 ^{o}C. It demonstrates that cyclic responses of both route-8E and route-8Bc UFG Ti are similar and at this temperature in spite of the fact that a slight improvement in both fatigue life and stress range values was observed in route-8B_c UFG Ti at the lowest strain amplitude. During monotonic tests of UFG Ti at room temperature, route B_c also displayed a gradual increase in strength values over route E although route E was found to provide the best combination of ductility and strength [11]. At room temperature, IF steel processed via route E and B_c showed noticeable cyclic stability despite the inferior response of materials processed via route A and C [35]. This was attributed to the formation of equiaxed fine grains and the larger volume fraction of HAGBs in materials processed via these efficient routes (routes E and B_c) [4,35]. As discussed earlier, HAGBs enhance cyclic stability leading to better fatigue performance.

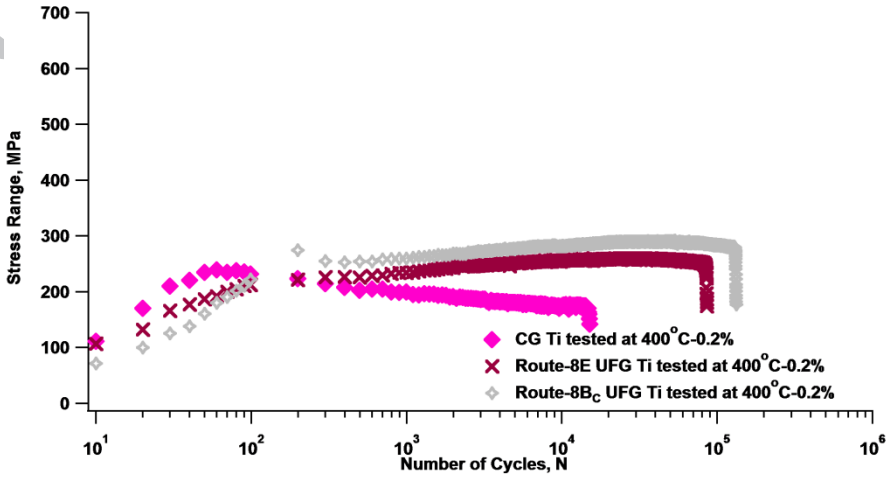

(a)

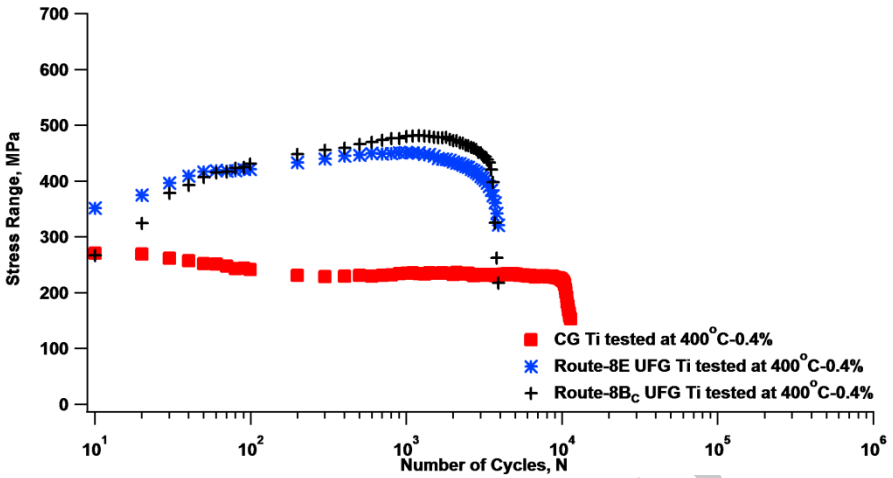

(b)

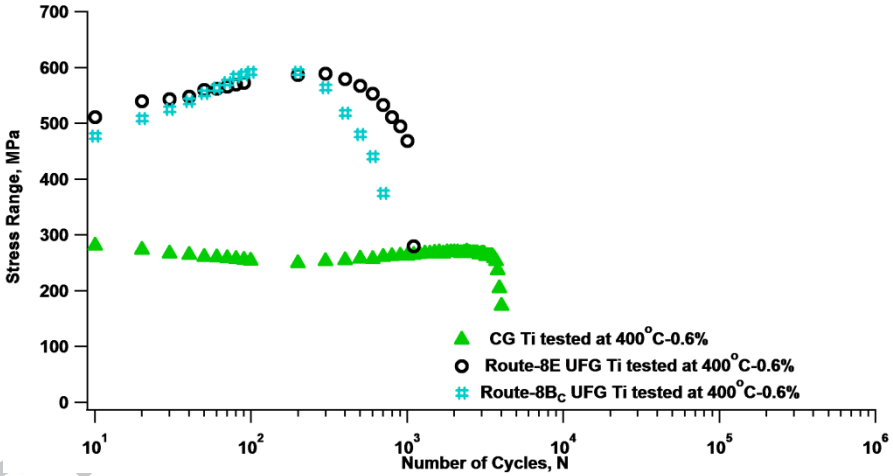

(c)

Figure 9. CDR of CG Ti, route-8E and route-8Bc UFG Ti at 400 °C with strain amplitudes of (a) 0.2% (b) 0.4% and (c) 0.6%

Route-8E and route-8B_c UFG Ti do not show better CDRs over CG Ti samples at 600 °C (Fig. 10). Owing to the occurrence of recrystallization and subsequent grain growth (see Fig. 6) at

such a high temperature, fatigue performance (i.e. fatigue life and stress range values) of severely deformed Ti is degraded, i.e. no considerable improvement in fatigue life and stress range values of severely deformed Ti as compared to that of the CG counterpart is seen. Regardless of the strain amplitude, stress range levels of CG Ti are equal or slightly higher than those of route-8B_c and route-8E severely deformed Ti. With respect to fatigue life, UFG Ti processed in both ECAE routes also could not surpass CG Ti. This confirms that the impacts of severe plastic deformation and processing routes on cyclic behavior of Ti are no longer significant at 600 ^{o}C.

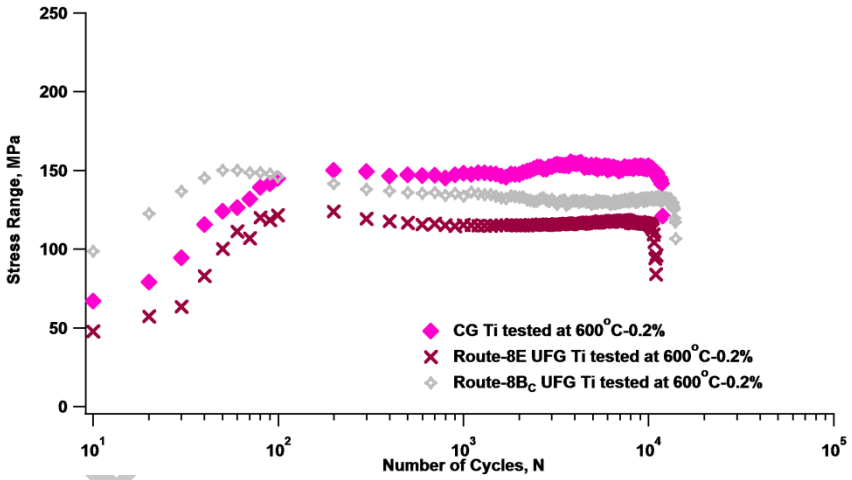

(a)

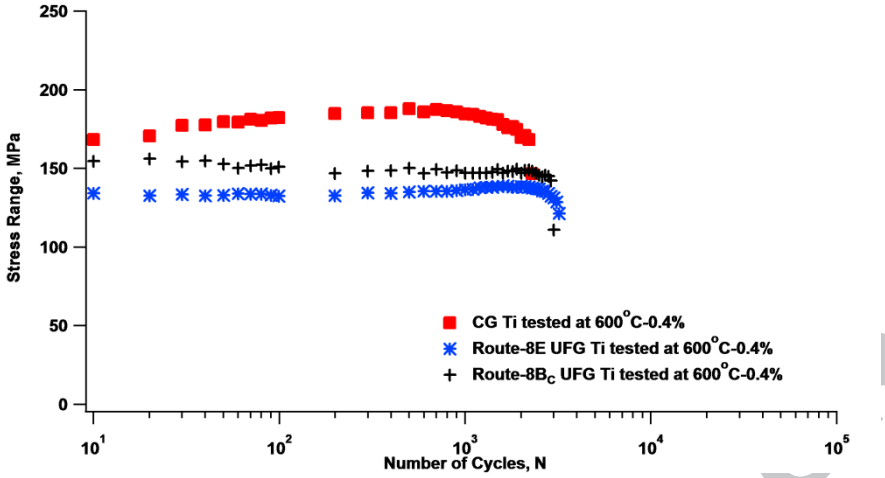

(b)

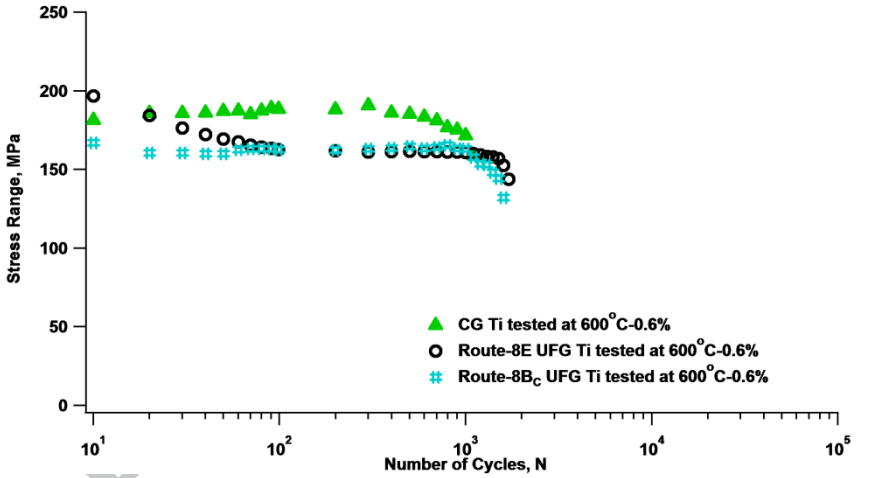

(c)

Figure 10. CDR of CG Ti, route-8E and route-8B_c UFG Ti at 600 ^{o}C with strain amplitudes of (a) 0.2% (b) 0.4% and (c) 0.6%

4. Conclusion

Cyclic deformation response and cyclic stability of severely deformed commercial purity grade 4 Ti were studied at both room and elevated temperatures (up to 600 ^{o}C) and at various

strain amplitudes. Influences of processing along route-8E and route-8Bc on the fatigue behavior of Ti were explored. The following conclusions can be drawn:

i. The LCF responses imply that ECAE processing is capable of improving the fatigue performance of grade 4 UFG Ti up to 400 ^{o}C (T_h = 0.35). For temperatures above 400 ^{o}C, cyclic stability of severely deformed Ti is worsened compared to the CG material. This behavior is associated with recrystallization, recovery and grain growth diminishing the positive effects of the initial UFG microstructure.

ii. Symmetric hysteresis loops were achieved for LCF experiments on both UFG and CG Ti. The amount of energy dissipation of UFG Ti was lower than that of CG Ti up to 400 ^{o}C, attesting better fatigue performance of UFG materials at these temperatures.

iii. Fatigue behavior of route-8E and route-8Bc UFG Ti appeared to be similar although materials processed via route B_c showed slightly higher fatigue life and stress range values at 400 ^{o}C.

Acknowledgements

Support from the EU-FP7 Marie Curie Career Integration Grant (304150-BUNSMAT) is acknowledged. Authors also thank the Hessen State Ministry of Higher Education, Research and the Arts - Initiative for the Development of Scientific and Economic Excellence (LOEWE) for support through the project 'Safer Materials'.

References

[1] Elias CN, Lima JHC, Valiev R, Meyers MA. Biomedical applications of titanium and its

alloys. JOM 2008;60:46–9. doi:10.1007/s11837-008-0031-1.

[2] Milner JL, Abu-Farha F, Bunget C, Kurfess T, Hammond VH. Grain refinement and mechanical properties of CP-Ti processed by warm accumulative roll bonding. Mater Sci Eng A 2013;561:109–17. doi:10.1016/j.msea.2012.10.081.

[3] Wang CT, Gao N, Gee MG, Wood RJK, Langdon TG. Processing of an ultrafine-grained titanium by high-pressure torsion: An evaluation of the wear properties with and without a TiN coating. J Mech Behav Biomed Mater 2013;17:166–75.

[4] Stolyarov V V, Zhu YT, Alexandrov I V, Lowe TC, Valiev RZ. Influence of ECAP routes on the microstructure and properties of pure Ti. Mater Sci Eng A 2001;299:59–67. doi:10.1016/S0921-5093(00)01411-8.

[5] Fan Z, Jiang H, Sun X, Song J, Zhang X, Xie C. Microstructures and mechanical deformation behaviors of ultrafine-grained commercial pure (grade 3) Ti processed by two-step severe plastic deformation. Mater Sci Eng A 2009;527:45–51. doi:10.1016/j.msea.2009.07.030.

[6] Purcek G, Saray O, Kul O, Karaman I, Yapici GG, Haouaoui M, Maier HJ. Mechanical and wear properties of ultrafine-grained pure Ti produced by multi-pass equal-channel angular extrusion. Mater Sci Eng A 2009;517:97–104. doi: 10.1016/j.msea.2009.03.054.

[7] Yapici GG, Karaman I, Maier HJ. Mechanical flow anisotropy in severely deformed pure titanium. Mater Sci Eng A 2006;434:294–302. doi:10.1016/j.msea.2006.06.082.

[8] Zhang S, Wang YC, Zhilyaev AP, Gunderov D V., Li S, Raab GI, et al. Effect of temperature on microstructural stabilization and mechanical properties in the dynamic testing of

nanocrystalline pure Ti. Mater Sci Eng A 2015;634:64–70. doi:10.1016/j.msea.2015.03.032.

[9] Niendorf T, Maier HJ, Canadinc D, Karaman I. Cyclic stability of ultrafine-grained interstitial-free steel at elevated temperatures. Mater Sci Eng A 2009;503:160–2. doi:10.1016/j.msea.2008.03.054.

[10] Mughrabi H, Höppel HW. Cyclic Deformation and Fatigue Properties of Ultrafine Grain Size Materials: Current Status and Some Criteria for Improvement of the Fatigue Resistance. MRS Proc 2000;634:B2.1.1. doi:10.1557/PROC-634-B2.1.1.

[11] Niendorf T, Canadinc D, Maier HJ, Karaman I, Yapici GG. Microstructure–mechanical property relationships in ultrafine-grained NbZr. Acta Mater 2007;55:6596–605. doi:10.1016/j.actamat.2007.08.015.

[12] Niendorf T, Canadinc D, Maier HJ, Karaman I. On the Microstructural Stability of Ultrafine-Grained Interstitial-Free Steel under Cyclic Loading. Metall Mater Trans A 2007;38:1946–55. doi:10.1007/s11661-007-9154-1.

[13] Semenova IP, Raab GI, Golubovskiy ER, Valiev RR. Service properties of ultrafine-grained Ti–6Al–4V alloy at elevated temperature. J Mater Sci 2013;48:4806–12. doi:10.1007/s10853-013-7305-x.

[14] Murashkin M, Sabirov I, Prosvirnin D, Ovid'ko I, Terentiev V, Valiev R, et al. Fatigue Behavior of an Ultrafine-Grained Al-Mg-Si Alloy Processed by High-Pressure Torsion. Metals (Basel) 2015;5:578–90. doi:10.3390/met5020578.

[15] Altan B. Severe plastic deformation : toward bulk production of nanostructured materials. Nova Science; 2006.

[16] Sordi VL, Ferrante M, Kawasaki M, Langdon TG. Microstructure and tensile strength of grade 2 titanium processed by equal-channel angular pressing and by rolling. J Mater Sci 2012;47:7870–6. doi:10.1007/s10853-012-6593-x.

[17] Sajadifar SV., Yapici GG. Elevated temperature mechanical behavior of severely deformed titanium. J Mater Eng Perform 2014;23:1834–44. doi:10.1007/s11665-014-0947-2.

[18] Shahmir H, Pereira PHR, Huang Y, Langdon TG. Mechanical properties and microstructural evolution of nanocrystalline titanium at elevated temperatures. Mater Sci Eng A 2016;669:358–66. doi:10.1016/j.msea.2016.05.105.

[19] Sajadifar S V., Yapici GG. Workability characteristics and mechanical behavior modeling of severely deformed pure titanium at high temperatures. Mater Des 2014;53:749–57. doi:10.1016/j.matdes.2013.07.057.

[20] Semenova IP, Korshunov AI, Salimgareeva GK, Latysh V V., Yakushina EB, Valiev RZ. Mechanical behavior of ultrafine-grained titanium rods obtained using severe plastic deformation. Phys Met Metallogr 2008;106:211–8. doi:10.1134/S0031918X08080140.

[21] Vinogradov AY, Stolyarov VV, Hashimoto S, Valiev RZ. Cyclic behavior of ultrafine-grain titanium produced by severe plastic deformation. Mater Sci Eng A 2001;318:163–73. doi:10.1016/S0921-5093(01)01262-X.

[22] Kim W-J, Hyun C-Y, Kim H-K. Fatigue strength of ultrafine-grained pure Ti after severe

plastic deformation. Scr Mater 2006;54:1745–50. doi:10.1016/j.scriptamat.2006.01.042.

[23] Semenova IP, Salimgareeva GK, Latysh VV, Lowe T. Enhanced fatigue strength of commercially pure Ti processed by severe plastic deformation. Mater Sci Eng A 2009;503:92–5. doi:10.1016/j.msea.2008.07.075.

[24] Czerwinski A, Lapovok R, Tomus D, Estrin Y, Vinogradov A. The influence of temporary hydrogenation on ECAP formability and low cycle fatigue life of CP titanium. J Alloys Compd 2011;509:2709–15. doi:10.1016/j.jallcom.2010.11.188.

[25] Niendorf T, Canadinc D, Maier HJ, Karaman I. The role of grain size and distribution on the cyclic stability of titanium. Scr Mater 2009;60:344–7.

[26] Wang YB, Li BQ, Sui ML, Mao SX. Deformation-induced grain rotation and growth in nanocrystalline Ni. Appl Phys Lett 2008;92:011903. doi:10.1063/1.2828699.

[27] Furnish TA, Mehta A, Van Campen D, Bufford DC, Hattar K, Boyce BL. The onset and evolution of fatigue-induced abnormal grain growth in nanocrystalline Ni–Fe. J Mater Sci 2017;52:46–59. doi:10.1007/s10853-016-0437-z.

[28] Segal VM. Engineering and commercialization of equal channel angular extrusion (ECAE). Mater Sci Eng A 2004;386:269–76. doi:10.1016/j.msea.2004.07.023.

[29] Li Q, Yu Q, Zhang J, Jiang Y. Effect of strain amplitude on tension–compression fatigue behavior of extruded Mg6Al1ZnA magnesium alloy. Scr Mater 2010;62:778–81. doi:10.1016/j.scriptamat.2010.01.052.

[30] Kumar A, Singh N, Singh V. Influence of stabilization treatment on low cycle fatigue behavior of Ti alloy IMI 834. Mater Charact 2003;51:225–33. doi:10.1016/j.matchar.2003.11.004.

[31] Lambers H-G, Rüsing CJ, Niendorf T, Geissler D, Freudenberger J, Maier HJ. On the low-cycle fatigue response of pre-strained austenitic Fe61Mn24Ni6.5Cr8.5 alloy showing TWIP effect. Int J Fatigue 2012;40:51–60. doi:10.1016/j.ijfatigue.2012.01.002.

[32] Mughrabi H, Höppel HW, Kautz M, Valiev RZ. Annealing treatments to enhance thermal and mechanical stability of ultrafine-grained metals produced by severe plastic deformation. Zeitschrift Für Met 2003;94:1079–83. doi:10.3139/146.031079.

[33] Canadinc D, Maier HJ, Gabor P, May J. On the cyclic deformation response of ultrafine-grained Al–Mg alloys at elevated temperatures. Mater Sci Eng A 2008;496:114–20. doi:10.1016/j.msea.2008.04.071.

[34] Rubitschek F, Niendorf T, Karaman I, Maier HJ. Microstructural stability of ultrafine-grained niobium–zirconium alloy at elevated temperatures. J Alloys Compd 2012;517:61–8. doi:10.1016/j.jallcom.2011.11.150.

[35] Niendorf T, Canadinc D, Maier HJ, Karaman I, Sutter SG. On the fatigue behavior of ultrafine-grained interstitial-free steel. Int J Mater Res 2006;97:1328–36. doi:10.3139/146.101377.

[36] Li SJ, Cui TC, Hao YL, Yang R. Fatigue properties of a metastable β-type titanium alloy with reversible phase transformation. Acta Biomater 2008;4:305–17.

doi:10.1016/j.actbio.2007.09.009.

[37] Lin Y-H, Hu K-H, Kao F-H, Wang S-H, Yang J-R, Lin C-K. Dynamic strain aging in low cycle fatigue of duplex titanium alloys. Mater Sci Eng A 2011;528:4381–9. doi:10.1016/j.msea.2011.02.013.

[38] Blum W, Li YJ, Durst K. Stability of ultrafine-grained Cu to subgrain coarsening and recrystallization in annealing and deformation at elevated temperatures. Acta Mater 2009;57:5207–17. doi:10.1016/j.actamat.2009.07.030.

[39] Wang SQ, Liu JH, Chen DL. Strain-controlled fatigue properties of dissimilar welded joints between Ti–6Al–4V and Ti17 alloys. Mater Des 2013;49:716–27. doi:10.1016/j.matdes.2013.02.034.

[40] Huang C, Zhao Y, Xin S, Tan C, Zhou W, Li Q, et al. High cycle fatigue behavior of Ti–5Al–5Mo–5V–3Cr–1Zr titanium alloy with lamellar microstructure. Mater Sci Eng A 2017;682:107–16. doi:10.1016/j.msea.2016.11.014.

[41] Huang C, Zhao Y, Xin S, Zhou W, Li Q, Zeng W, et al. High cycle fatigue behavior of Ti–5Al–5Mo–5V–3Cr–1Zr titanium alloy with bimodal microstructure. J Alloys Compd 2017;695:1966–75. doi:10.1016/j.jallcom.2016.11.031.

[42] Shyam A, Lara-Curzio E. A model for the formation of fatigue striations and its relationship with small fatigue crack growth in an aluminum alloy. Int J Fatigue 2010;32:1843–52. doi:10.1016/j.ijfatigue.2010.05.005.

[43] Kitahara H, Uchikado K, Makino J, Iida N, Tsushida M, Tsuji N, et al. Fatigue Crack

Propagation Behavior in Commercial Purity Ti Severely Deformed by Accumulative Roll Bonding Process. Mater Trans 2008;49:64–8. doi:10.2320/matertrans.ME200716.

[44] Mirzakhani B, Salehi MT, Khoddam S, Seyedein SH, Aboutalebi MR. Investigation of Dynamic and Static Recrystallization Behavior During Thermomechanical Processing in a API-X70 Microalloyed Steel. J Mater Eng Perform 2009;18:1029–34. doi:10.1007/s11665-008-9338-x.

[45] Monk J, Farkas D. Strain-induced grain growth and rotation in nickel nanowires. Phys Rev B 2007;75:045414. doi:10.1103/PhysRevB.75.045414.

[46] Haslam A., Phillpot S., Wolf D, Moldovan D, Gleiter H. Mechanisms of grain growth in nanocrystalline fcc metals by molecular-dynamics simulation. Mater Sci Eng A 2001;318:293–312. doi:10.1016/S0921-5093(01)01266-7.

[47] Zhang Y, Tucker GJ, Trelewicz JR. Stress-assisted grain growth in nanocrystalline metals: Grain boundary mediated mechanisms and stabilization through alloying. Acta Mater 2017;131:39–47. doi:10.1016/J.ACTAMAT.2017.03.060.

[48] Sakai T, Jonas JJ. Overview no. 35 Dynamic recrystallization: Mechanical and microstructural considerations. Acta Metall 1984;32:189–209. doi:10.1016/0001-6160(84)90049-X.

Highlights

1. Fatigue of UFG Ti at temperatures up to 600C is investigated.

2. Effect of processing route is investigated.

3. Improved fatigue performance up to 400C is demonstrated.

4. Strain path does not have strong affect on the fatigue behavior when comparing routes Bc and E.